Journal of the mechanical behavior of biomedical materials 67 (2017) 40–50

Contents lists available at ScienceDirect

Journal of the Mechanical Behavior of Biomedical Materials

journal homepage: www.elsevier.com/locate/jmbbm

Rifle bullet penetration into ballistic gelatin

Yaoke Wen[a,*], Cheng Xu[a], Yongxi Jin[b], R.C. Batra[c]

[a] School of Mechanical Engineering, Nanjing University of Science and Technology, Nanjing 210094, China
[b] No.208 Research Institute of China Ordnance Industries, Beijing 102202, China
[c] Department of Biomedical Engineering and Mechanics, M/C 0219, Virginia Polytechnic Institute and State University, Blacksburg, VA 24061, USA

ARTICLE INFO

Keywords:
Ballistic gelatin
Temporary cavity
Rifle bullet
Penetration
Angle of attack

ABSTRACT

The penetration of a rifle bullet into a block of ballistic gelatin is experimentally and computationally studied for enhancing our understanding of the damage caused to human soft tissues. The gelatin is modeled as an isotropic and homogeneous elastic-plastic linearly strain-hardening material that obeys a polynomial equation of state. Effects of numerical uncertainties on penetration characteristics are found by repeating simulations with minute variations in the impact speed and the angle of attack. The temporary cavity formed in the gelatin and seen in pictures taken by two high speed cameras is found to compare well with the computed one. The computed time histories of the hydrostatic pressure at points situated 60 mm above the line of impact are found to have "two peaks", one due to the bullet impact and the other due to the bullet tumbling. Contours of the von Mises stress and of the effective plastic strain in the gelatin block imply that a very small region adjacent to the cavity surface is plastically deformed. The angle of attack is found to noticeably affect the penetration depth at the instant of the bullet tumbling through 90°.

1. Introduction

Ballistic gelatin, hereafter referred to as gelatin, is often used as a simulant for studying impact damage in soft biological tissues (Maiden, 2009; Nicholas and Welsch, 2004). Gelatin, a protein derived from either skin or bone (Kneubuehl, 2011), is produced by submitting collagen to an irreversible process that renders it water-soluble. Two common gelatin formulations, 10% by mass at 4 °C and 20% by mass at 10 °C, are often used by researchers (Nicholas and Welsch, 2004; Jussila, 2004); henceforth “by mass” is omitted for brevity when describing the gelatin. For simulating the impact of a projectile into gelatin one needs its material properties over the range of strains, strain-rates and temperatures likely to occur at anticipated impact velocities.

Cronin and Falzon (2010) studied effects of temperature, ageing time and strain-rate on 10% gelatin, and found that upon increasing the strain-rate to 1/s the failure stress modestly increased. By using an MTS machine and a modified split Hopkinson pressure bar, the uniaxial compressive stress–strain response of 10% gelatin under quasi-static and dynamic (strain-rate of 1,000–5,200/s) loading were measured by three different research groups. While Richler and Rittel's (2014) results show that there is a high strain-rate dependence even at low strain rates, Kwon and Subhash (2010) found that the gelatin strength remained essentially constant at strain rates representative of the quasi-static regime. Salisbury and Cronin's (2009) results agree with those of Richler and Rittel at high strain rates but disagree with those of Kwon and Subhash at very low strain rates. Moy et al. (2010) tested gelatin in uniaxial tension and found that the response also exhibited strain-rate dependence and the failure stress increased with an increase in the strain-rate.

Aihaiti and Hemley (2008) have shown that Poisson's ratio of 10% gelatin increases from 0.34 to about 0.37 when the pressure is increased from 0 to around 3 GPa, and stays at 0.37 for pressures between 3 and 12 GPa. Nagayama et al. (2006) have presented shock Hugoniot compression data for several bio-related materials by using flat plate impact experiments, and for the 10% gelatin have proposed the following relation

$$U_S = 1.52 + 2v_p \tag{1}$$

In Eq. (1) U_S and v_p are the shock and the particle speed, respectively. Appleby-Thomas et al. (2011) also employed plate-impact experiments to study the dynamic response of 25% gelatin, ballistic soap and lard. These three materials exhibited linear Hugoniot $U_S - v_p$ relations. Whereas the gelatin behaved hydrodynamically under shock, the soap and the lard appeared to strengthen under increased loading.

Mechanisms dominating deformations of solids generally vary with the impact speed. Wilbeck (1978) has classified deformations of some low strength materials (birds, gelatin and RTV rubber) into five

* Corresponding author.
E-mail address: wenyk2011@163.com (Y. Wen).

http://dx.doi.org/10.1016/j.jmbbm.2016.11.021
Received 27 June 2016; Received in revised form 26 November 2016; Accepted 29 November 2016
Available online 02 December 2016
1751-6161/

regimes: elastic, plastic, hydrodynamic, sonic and explosive. There is no single constitutive relation for gelatin that well describes its mechanical behavior in all these five regimes. For low velocity impact a rate-dependent hyperelastic constitutive model is expected to describe well the mechanical behavior of gelatin (Wen et al., 2015). However, for high velocity impact the hydrodynamic response that considers possible phase transformations may be more suitable (Wen et al., 2013; Johnson and Holzapfel, 2006). The strength of the gelatin may play a significant role once the penetrator has considerably slowed down.

Koene and Papy (2010) used the software AUTODYN to study deformations induced by the penetration of Acrylonitrile-Butadiene-Styrene plastic spheres into gelatin at speeds up to 160 m/s. For simulating tests of armor impacting gelatin, Shen et al. (2010) modeled gelatin as nearly incompressible rubber. Cronin (2011) employed a viscoelastic material model, and Cronin and Falzon (2009) a rate-dependent hyperelastic model by using tabulated values of stresses and strains. It was found that the viscoelastic material model could adequately capture only the low strain-rate response of the gelatin, and the tabulated hyperelastic model well represented deformations of the gelatin at low and intermediate strain rates. However, high strain rates of the order of 1,000/s were not considered. Hub et al. (2012) used the Smooth Particle Hydrodynamics method with gelatin's response represented by a modified material model for water, and found the volume of the computed cavity to be much larger than that of the cavity developed during the tests. Wen et al. (2013) simulated the sphere-10% gelatin interaction at high impact velocities with an elastic-plastic hydrodynamic material model and a polynomial equation of state (EoS). Their computed evolution of a temporary cavity and time histories of the pressure agreed well with test findings. Yoon et al. (2015) adopted a rate-dependent shear model with the Mie-Gruneisen EoS to define the gelatin behavior for impact with a handgun bullet.

This article presents experimental and numerical (using the commercial software, LS-DYNA) approaches to study the interaction between a rifle bullet and a gelatin block. Two high-speed cameras are used to capture the cavity profiles in the vertical and the horizontal directions. The gelatin is modeled as an elastic-plastic material with linear strain-hardening and a cubic polynomial relation between the hydrodynamic pressure and the change in mass density. Effects of uncertainties in the impact speed and the angle of attack are quantified. The computed penetration depth and cavity profiles are found to agree well with the corresponding experimental results. Time histories of the kinetic energies of the bullet and the gelatin show two inflection points in each curve, one corresponding to the bullet tumbling through 90° and the other to the bullet exiting the gelatin. It is found that only a small region of the gelatin adjacent to the surface of the cavity formed in the gelatin is plastically deformed, and the angle of attack noticeably affects the time when the bullet tumbles.

2. Experimental results

A 300 mm×300 mm×300 mm gelatin (10% by mass at 4 °C) block resting on a table was impacted by a 7.62 mm diameter bullet using a rifle with its muzzle 100 m from the front face of the gelatin that was prepared using the procedure proposed by Jussila (2004). The 7.62 mm×39 mm bullet we used is the 1956 7.62 mm ball ammunition (China) and is an imitation of the Soviet 7.62 mm×39 mm M43 ammunition for the AK47 assault rifle. The bullets were manufactured in 2012 by the Heilongjiang North Tool Co., Ltd., China. The manufacturer did not provide details of the composition and the hardness of bullet components.

The 300 mm×300 mm×300 mm gelatin block is the Chinese Military Standard because this size is deemed to be close to that of a human upper torso. For the 300 mm×300 mm×300 mm 10% (by mass) gelatin block, 24.3 kg water at room temperature and 2.7 kg gelatin powder were used. The dependence of water density upon the

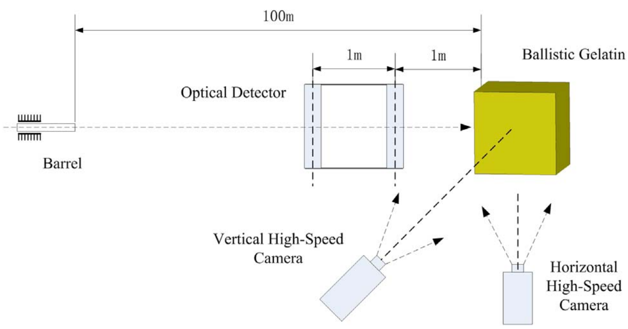

Fig. 1. Schematics of the experimental set-up.

temperature was ignored. The material properties of the ballistic gelatin depend upon the temperature. The gelatin block was stored in a chamber at 4 °C prior to testing, and the test was conducted within 3 min of taking the block from the chamber. We did not check the gelatin temperature after the test.

The maximum size of the temporary cavity for most tests was about 200 mm. The block width and the block height equal nearly 40 times the bullet diameter implying that boundary conditions at the edges will have very little effect on the gelatin/bullet interaction. The speed of the bullet just before impacting the gelatin was measured with a double base optical detector with two grating lines 1 m apart and the detector located 1 m from the front face of the gelatin as shown in Fig. 1. Two high-speed cameras capable of taking 15,000 frames per second with a resolution of 600×600 pixels were used to capture the size and the location of the temporary cavity from the vertical and the horizontal directions (Fig. 1). The appropriate lighting was used to increase block's transparency and vividly visualize the ballistic phenomena.

An item of interest during the penetration of the bullet into the gelatin is the formation of the temporary cavity. The kinetic energy (KE) of the bullet transferred to the gelatin accelerates the medium surrounding the bullet path and moves the gelatin away from the bullet both radially and axially thereby creating a tunnel called a temporary cavity. Photographs at different times revealing the evolution of the temporary cavity in the vertical and the horizontal directions in the gelatin impacted by the bullet moving at 625 m/s are exhibited in Fig. 2. The muzzle velocity of a 7.62 mm×39 mm bullet is typically 710 m/s - 730 m/s. However, the optical detector in our experiments measured the average velocity of the bullet to be 625 m/s which could be due to the firing distance of ~100 m. The experiments were replicated three times. Results in two tests were close to each other but in the third one there was a very long neck length.

At 0.2 ms after impact, a slim cone can be seen in the left-half of the gelatin block and the cone is transformed into a cylindrical shaped narrow channel at t =1.6 ms. However, at a later time of ~5 to 6 ms, the tumbling motion of the bullet results in a nearly ellipsoidal cavity having principal diameters of ~175 mm and 185 mm in the horizontal and the vertical directions, respectively. The maximum diameter of the cavity is ~24 times that of the bullet. Subsequently, the cavity springs back due to the recovery of elastic deformations reaching its minimum diameters, respectively, of 84 mm and 97 mm in the horizontal and the vertical directions at ~11 ms.

The time histories of the temporary cavity diameters in the vertical and the horizontal directions determined from the high-speed photographs are exhibited in Fig. 3. For results of 625 m/s impact velocity, the greater cavity diameter in the vertical direction than that in the horizontal direction suggests that the bullet tumbles in the vertical plane. This can also be seen by comparing cavity shapes in the vertical and the horizontal directions at 1.6 ms in Fig. 2. For the 629 m/s impact velocity, the cavity diameters in the vertical and the horizontal directions are close to each other. It indicates that the bullet tumbling plane is inclined at ~45° with the vertical plane. The maximum and the minimum diameters of the temporary cavity may be influenced by the

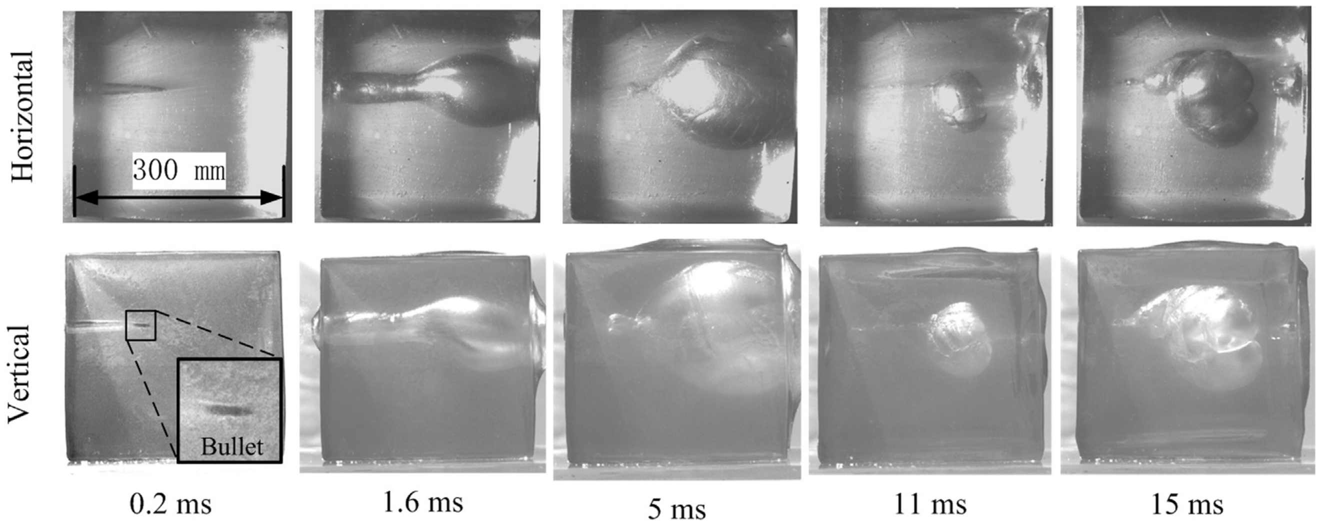

Fig. 2. Temporary cavity evolution in the vertical and the horizontal directions captured by the high-speed cameras.

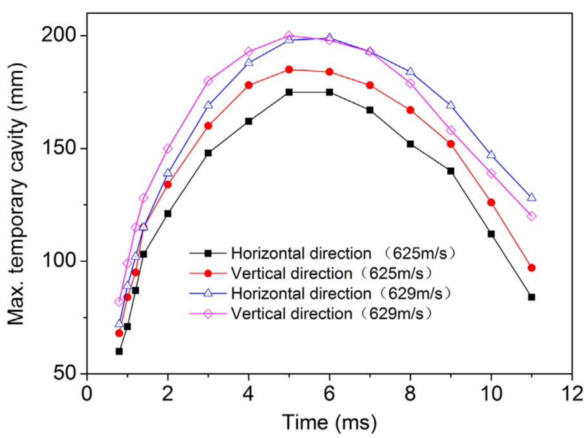

Fig. 3. Time histories of the cavity diameters in the vertical and the horizontal directions.

300 mm×300 mm×300 mm size of the gelatin block.

3. Computational results

3.1. Finite element mesh and material model

Numerical simulations using a verified computer code and a validated mathematical model provide details of deformations that may not be experimentally measureable. Here the finite element (FE) based commercial software, LS-DYNA, is used to simulate as closely as possible the test conditions and computing 3-dimensional (3-D) deformations of the gelatin impacted by the bullet. The bullet spin is ignored, and the initial angle of attack when the bullet impacts the gelatin is assumed since it could not be measured in the tests. As discussed in Section 4.5 it noticeably affects the bullet motion in the gelatin. The numerical results with an initial angle of attack of 1° were found to agree well with the corresponding experimental observations. The bullet geometry used here is recommended by the No. 208 Research Institute of China Industries. The discretization of the bullet and the gelatin into FEs is depicted in Fig. 4. The half model with the YZ-plane as the symmetry plane was used to reduce the computation time. The key word CONSTRAINED_GLOBAL in LS-DYNA was used to impose displacement constraints on the symmetry plane. The outside surfaces are traction free and the contact surface between the gelatin and the table is assumed to be frictionless.

The gelatin is modeled as an elastic-plastic linearly strain-hardening material with the polynomial EoS, Eq. (5), and the yield strength, σ_y, given by (Hallquist, 2012)

$$\sigma_y = \sigma_0 + E_h \bar{\varepsilon}^p \tag{2}$$

where σ_0 is the initial yield strength, $\bar{\varepsilon}^p$ the effective plastic strain,

$$E_h = \frac{E_t E}{E - E_t} \tag{3}$$

the plastic hardening modulus, E Young's modulus, and E_t the tangent modulus. The material is assumed to obey the von Mises yield criterion

$$\phi = \frac{1}{2} s_{ij} s_{ij} - \frac{\sigma_y^2}{3} = 0 \tag{4}$$

where $s_{ij}$is the deviatoric stress tensor.

Constitutive relations (2) – (4) are supplemented with the following polynomial EoS relating the pressure,p, with the change in the specific volume or the mass density ρ (Wilbeck, 1978; Wang et al., 2009):

$$p = C_0 + C_1\mu + C_2\mu^2 + C_3\mu^3 \tag{5}$$

where $\mu = (\rho/\rho_0 - 1)$ is a dimensionless parameter defined in terms of the ratio of the current mass density ρ to the initial mass density ρ_0, and C_0, C_1, C_2 and C_3 are material constants. Wilbeck (1978) has shown that the pressure-density relation across a shock wave can be written as

$$p = \frac{\rho_0 c_0^2 \eta}{(1 - k\eta)^2}, \quad \eta = 1 - \frac{\rho_0}{\rho} = \frac{\mu}{1 + \mu} \tag{6}$$

where the Hugoniot parameter k is a constant. For small to moderate values of μ Johnson and Holzapfel (2003, 2006) have shown that Eq. (6) reduces to Eq. (5) with $C_0 = 0$, $C_1 = \rho_0 c_0^2$, $C_2 = (2k - 1)C_1$ and $C_3 = (k - 1)(3k - 1)C_1$. Thus if we know values of k (2 for 10% gelatin) and either of the bulk modulus C_1 or of the sound speed c_0 (1520 m/s for 10% gelatin) then constants C_2 and C_3 can be evaluated (Nagayama et al., 2006). Values of material parameters for the gelatin used in this work are listed in Table 1. Since the value of C_1 is much greater than that of E, therefore the gelatin mass density does not change much during deformations.

The Johnson-Cook constitutive relation is used to simulate the response of the bullet materials, and values of the material parameters are listed in Table 2.

3.2. Effect of finite element mesh refinement

For the 625 m/s impact velocity and the 1° initial angle of attack, deformations of the bullet and the development of temporary cavity profiles in the gelatin were analyzed by using three FE meshes depicted

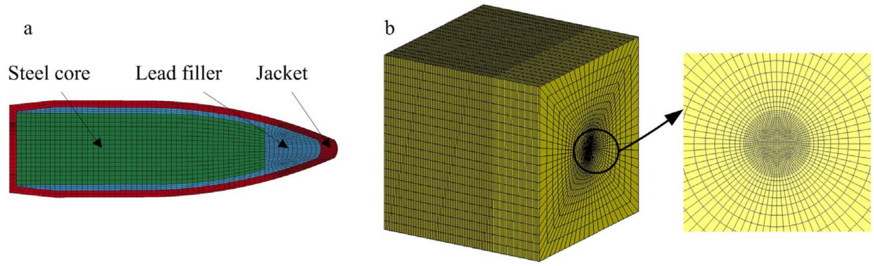

Fig. 4. Discretization of the 7.62 mm bullet and the gelatin block into finite elements.

in Fig. 5. The volume of an element for the coarse, the fine and the finest FE mesh for the gelatin in the impacted area is 0.45, 0.2 and 0.1 mm^3, respectively.

For t=0.2 and 0.6 ms, the computed temporary cavity profiles in the gelatin for the three FE meshes are shown in Fig. 6. The temporary cavity looks like a slender cone at 0.2 ms, and the computed penetration depth of the bullet is nearly the same for the three FE meshes. For the finest mesh the bullet has tilted a little more than that for the other two meshes. At 0.6 ms the temporary cavity looks like a cylinder for the three FE meshes, and the bullet tumbling angles equal ~75.6°, 145° and 162.5°, respectively, for the coarse, the fine and the finer FE meshes. Whereas the tumbling angles for the coarse and the fine FE meshes noticeably differ, those for the fine and the finer meshes are close to each other. The cavity length is a little longer and the cavity diameter is a little smaller for the coarse mesh than those for the other two meshes. Unless otherwise mentioned, results reported below are for the fine mesh since significantly less computational resources are needed for it than those for the finer mesh.

3.3. Comparison of results for rigid and deformable bullets

We first investigate differences in the results computed with and without considering deformations of the bullet materials. Time histories of the tumbling angle and of the bullet speed depicted, respectively, in Figs. 7 and 8 for the rigid and the J-C material models reveal that the tumbling angle at 0.6 ms and the penetration speed from 0.3 to 0.5 ms for the former is 6.5% more and 5.5% less than those for the latter. Otherwise, the time histories for the rigid and the J-C material models agree with each other. However, assuming the bullet to be rigid did not noticeably save computational resources. Thus the J-C material model is used for the bullet materials in the results reported below. Results exhibited in Fig. 8 reveal that till 0.45 ms the computed bullet velocity by regarding it as either rigid or modeling it by the Johnson-Cook material is very close to that experimentally observed. However, beyond 0.45 ms, the two computed bullet velocities are still close to each other but they differ from the experimental one. The residual velocities of the bullet upon exiting from the gelatin equal 343, 275 and 276 m/s, respectively, from the test data, the J-C material and the rigid material for the bullet. We note that Antoine and Batra (2016) have reported that for the polycarbonate target, modeling the penetrator as rigid rather than by the Johnson-Cook material model significantly reduced the computational resources needed to study the perforation problem.

As the bullet penetrates into the gelatin the bullet nose radially pushes out the gelatin. The speed of the gelatin particles and hence dimensions of the temporary cavity at that location depend on the instantaneous KE transferred to the gelatin. During the first 0.45 ms of impact nearly 60% of the bullet KE has been transferred to the gelatin. Due to the reduction in the bullet speed and its KE, the radial speed of gelatin particles pushed away by the bullet is quite different for t > 0.45 ms from what it was for t < 0.45 ms. This influences dimensions of the temporary cavity at the exit position.

The error in measuring the bullet residual velocity from the high speed video images is larger than that in assessing the temporary cavity size.

Values of material parameters in the elastic-plastic hydrodynamic model used to simulate the response of the 10% gelatin have been deduced by the inverse technique of minimizing the error between the computed and the experimental cavity sizes. Thus the numeric model predicts the cavity size better than the residual velocity. Furthermore, we found that the present material model with the EoS predicts well the high velocity impact (300–1000 m/s) of gelatin. However, it does not do that well for low velocity impact for which a rate-dependent hyperelastic model is recommended. We note that Batra and Kim (1990) used an inverse technique to identify material parameters for a thermo-elasto-visco-plastic material.

3.4. Effect of interface friction

For high speed impacts of hard objects on soft targets, the penetration resistance is mainly influenced by the EoS of the target and the penetrator nose shape with frictional forces generally having negligible effects. In an attempt to show that it also holds for the present impact problem, we have assumed that the Coulomb friction law applies and have plotted in Fig. 9 time histories for three values of the coefficient of friction of the total contact force acting on the bullet impacting at 625 m/s and an angle of attack of 1°. These plots reveal that the interface friction has a negligible effect on the bullet retardation. The consideration of frictional forces did not noticeably affect the distribution of the effective plastic strain in the region adjoining the bullet/gelatin interface, and the penetration depth.

Chen and Batra (1993) and Batra and Chen (1994) have deduced frictional force as a function of the relative velocity between the two sliding bodies and shown that the penetration depth into deep targets is influenced by the frictional force.

3.5. Sensitivity of computed results to impact speed

In order to quantify the sensitivity of results to the impact speed, we have studied the problem for the following five impact speeds, 624.7000, 624.9997, 625.0000, 625.0003 and 625.3000 m/s as suggested by Anderson and Holmquist (2013a, 2013b) and Chadegani et al. (2015). For the hypervelocity impact of a 0.5 mm diameter steel sphere on a flat sheet of fused silica glass Chadegani et al. (2015)

Table 1
Values of material parameters for the gelatin.

ρ (kg/m^3)	E (kPa)	E_t (kPa)	σ_0 (MPa)	C_0 (GPa)	C_1 (GPa)	C_2 (GPa)	C_3 (GPa)
1,030	850	10	0.22	0	2.38	7.14	11.9

Table 2
Values of the Johnson-Cook material parameters for the bullet components.

	ρ (g/cm^3)	G (GPa)	T (K)	T_m (K)	A (MPa)	B (MPa)	n	C	m
Jacket	7.92	77	293	1793	792	510	0.014	0.28	1.03
Lead filler	11.34	7	293	600	14	17.6	0.685	0.035	1.68
Steel core	7.83	77	293	1793	792	510	0.014	0.28	1.03

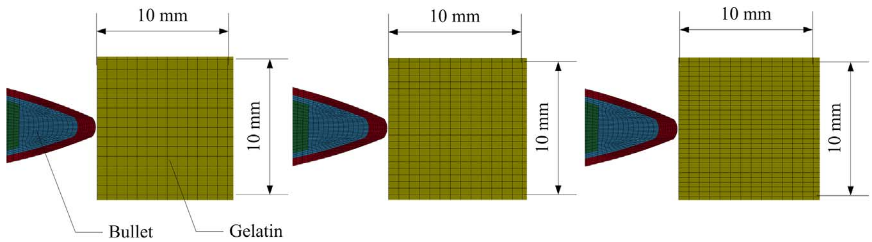

Fig. 5. Enlarged views of the coarse (left), the fine (center) and the finer (right) FE mesh for a small portion near the impacted region of the gelatin.

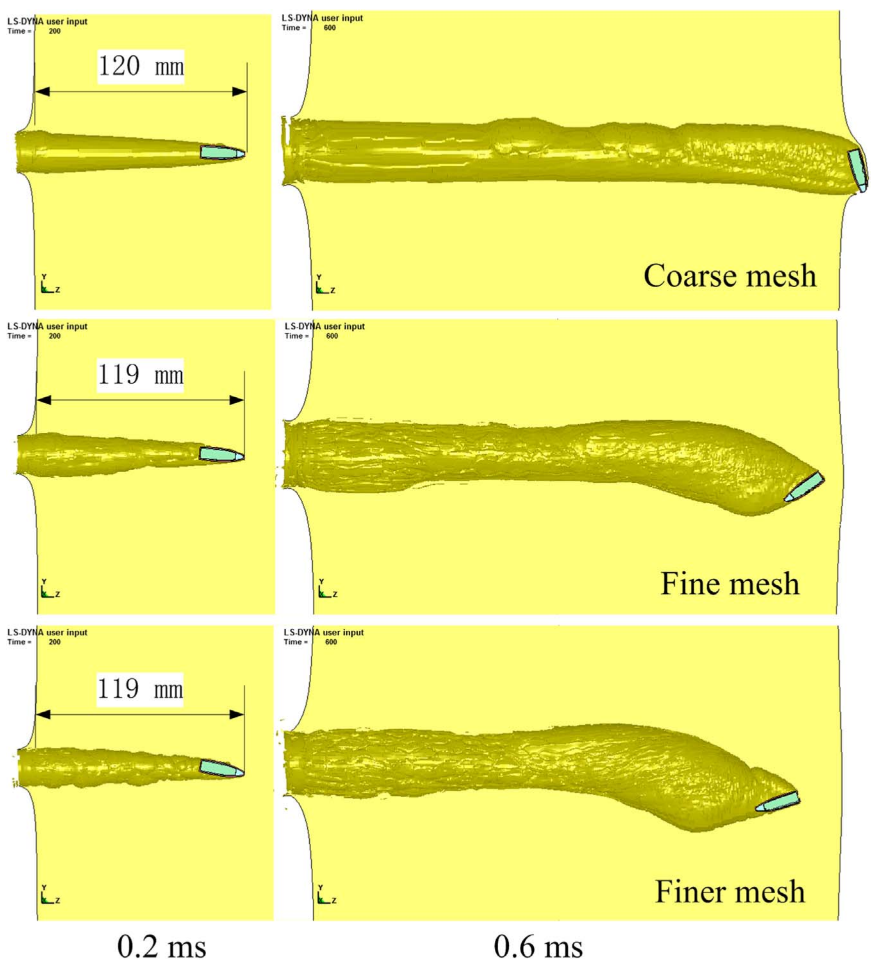

Fig. 6. For the three FE meshes, temporary cavity profiles in the gelatin and the bullet orientations at 0.2 and 0.6 ms.

conducted sensitivity studies by varying the impact speed from 3,000 m/s to 3000.0001, 3000.0002 and 3000.003 m/s. They found essentially no change in the failure characteristics of the fused silica panel. Furthermore, values of crack lengths and conchoidal diameters smoothly changed when the impact speed was varied between 2.99 and 3.01 km/s. However, while studying the response of glass targets to impact by small impactors, Anderson and Holmquist (2013a, 2013b) found that for impact velocities of 2238, 2238.0001, 2238.0002, 2066 and 2066.0001 m/s, the computed penetrator/target front position significantly varied. For example, for 0.0001 m/s or 5×10^{-6} % increase in the impact velocity, the final depth of the failure and the penetration fronts increased by about 20% and more than 10%, respectively, showing high sensitivity of the computational model to the impact speed. They did not give any reasons for such large variations in the position front for tiny variations in the impact speed. Chadegani et al. (2015) and Anderson and Holmquist (2013a, 2013b) employed different software. Without having the source code it is difficult to pinpoint what is causing this high sensitivity to tiny variations in the impact velocity. Generally speaking, “if or conditional statements” in a code can pass or fail with a small variation in the input parameters. The

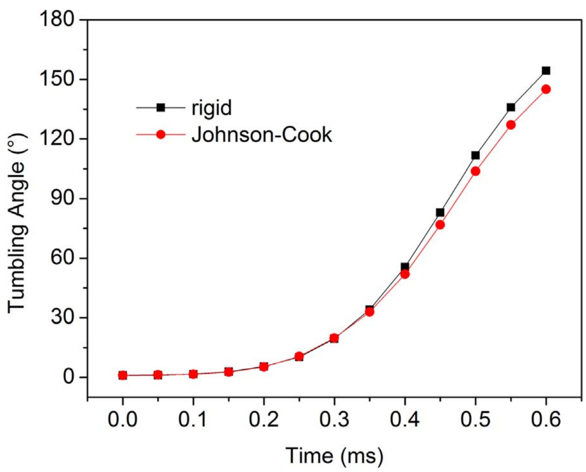

Fig. 7. Time histories of the tumbling angle for the bullet modeled as rigid and the J-C material.

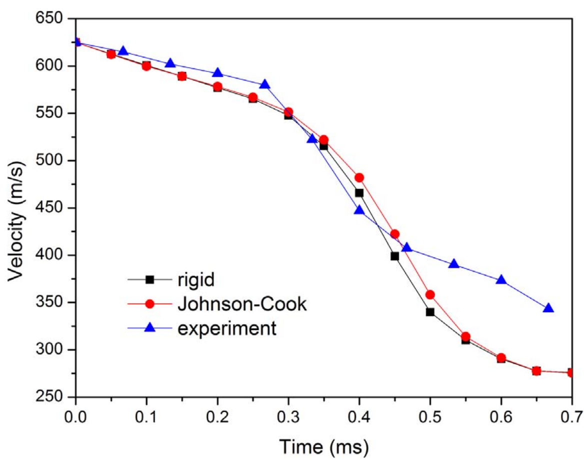

Fig. 8. Time histories of the computed and the experimental residual velocities for the bullet.

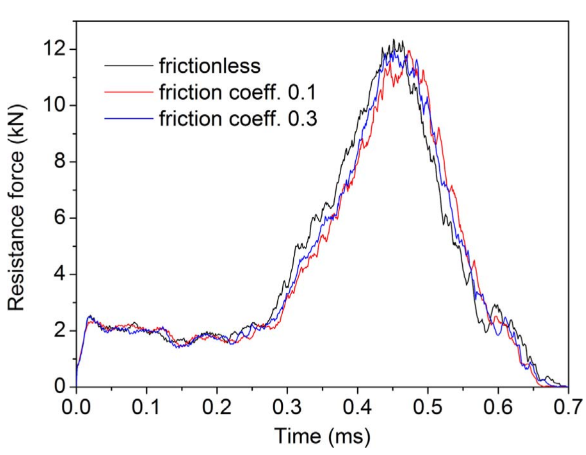

Fig. 9. Time histories of the impactor contact force for three values of the coefficient of friction for the 7.62 mm bullet impacting the gelatin block at 625 m/s and the angle of attack of 1°.

most often causes of this sensitivity are plastic yielding and material failure at a point.

The residual speed and the tumbling angle of the bullet at 0.7 ms and the gelatin temporary cavity size (D_{NC} and D_{TC} in Fig. 10) at 2 ms for these impact speeds are summarized in Table 3. The cavity shape for the 625.0000 m/s impact speed is depicted in Fig. 9. It is interesting to note that the minute change, ± 0.0003 m/s, in the impact speed has

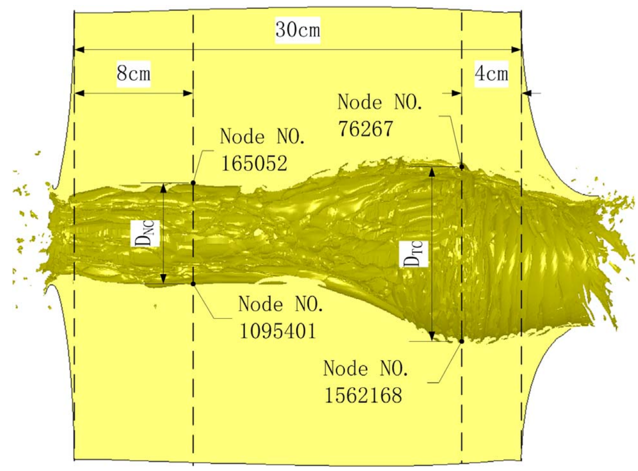

Fig. 10. Approximate temporary cavity size at 2 ms for impact speed of 625 m/s.

Table 3
Values of penetration characteristics for five different impact speeds.

Impact velocity(m/s)	Bullet @ 0.7 ms		Gelatin @ 2 ms	
	Residual velocity(m/s)	Tumbling angle (°)	D_{NC} (mm)	D_{TC} (mm)
624.7000	276.40	169.46	67.88	124.21
624.9997	281.26	170.55	67.17	118.52
625.0000	275.46	170.22	67.98	118.20
625.0003	272.29	171.50	67.52	119.59
625.3000	276.17	167.29	68.15	125.98

Table 4
Values of penetration characteristics for three slightly different angles of attack.

Angle of attack (°)	Bullet @ 0.7 ms		Gelatin @ 2 ms	
	Residual velocity (m/s)	Tumbling angle (°)	D_{NC} (mm)	D_{TC} (mm)
0.9997	279.14	172.09	67.76	118.11
1.0000	275.46	170.22	67.98	118.20
1.0003	264.34	167.86	67.39	117.76

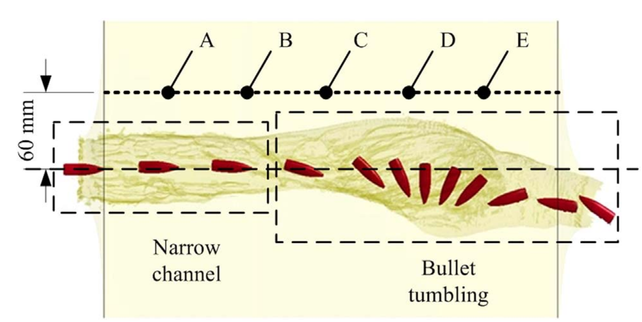

Fig. 11. Computed bullet trajectory and locations of points, 50 mm apart, where the computed pressure is reported.

greater percentage influence on the residual velocity of the bullet than the 1000 times larger change, ± 0.3 m/s. For example, for impact speeds of 624.9997 and 624.7 m/s (or 0.00005% and 0.048% different from 625 m/s), the residual bullet speed at 0.7 ms changed by 2.1% and 0.3%, respectively, as compared to that with the impact speed of 625 m/s. However, the change, ± 0.3 m/s (or 0.048%), in the impact speed has greater influence on the D_{TC} in the gelatin than the ± 0.0003 m/s (or 0.00005%) change in the impact speed. The tumbling angle of the bullet and the value of D_{NC} in the gelatin change very little

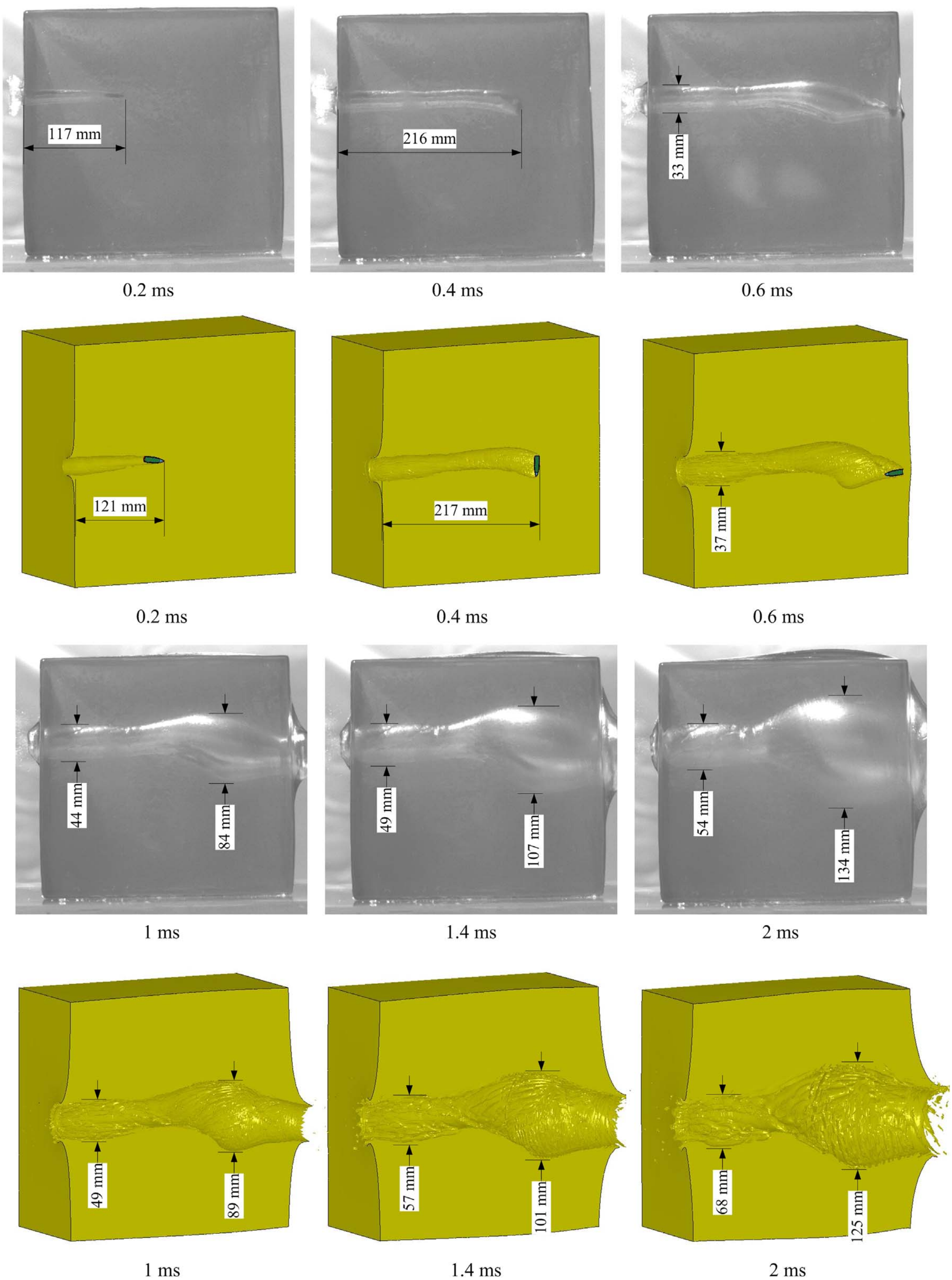

Fig. 12. Comparison of the computed and the experimentally observed temporary cavity shapes.

for infinitesimal variations in the impact speed. These results suggest that computations are sensitive to a tiny change in the impact speed but seem stable and give useful information for designing experiments and ascertaining damage to soft tissues.

3.6. Sensitivity to the angle of attack

For the three angles of attack equal to 0.9997°, 1° and 1.0003°, and the 625 m/s impact speed, numerical results summarized in Table 4 suggest that the residual velocity and the tumbling angle of the bullet are more sensitive to infinitesimal changes in the angle of attack than the values of D_{NC} and D_{TC} for the temporary cavity formed in the gelatin. For example, for the angle of attack =1.0003°, the residual velocity and the tumbling angle of the bullet at 0.7 ms changed by 4.0% and 1.4%, respectively, as compared with those for the angle of attack of 1°. However, values of D_{NC} and D_{TC} in the gelatin changed by less

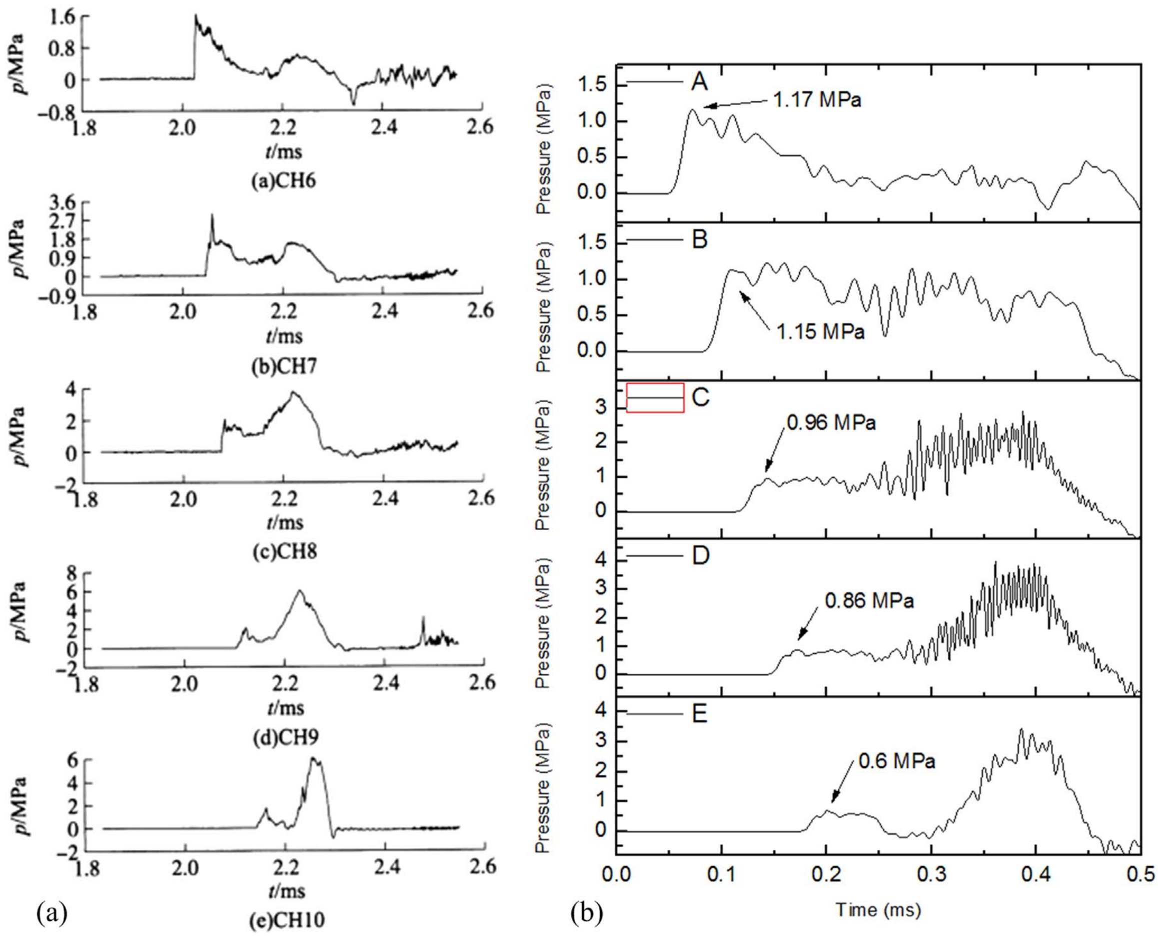

Fig. 13. Time histories of the (a) experimental pressure in the gelatin for the 5.56×45 mm rifle bullet from Huang et al. (2013), and of (b) presently computed pressure in the gelatin for the 7.62×39 mm rifle bullet.

than 1%.

4. Numerical results and discussion

4.1. Bullet motion and trajectory

The computed bullet trajectory in the gelatin is exhibited in Fig. 11. As mentioned earlier, bullet's deformations observed in tests and computations were negligible. After penetration into the gelatin, the bullet moves steadily for about 100 mm before a marked tumbling motion is observed and a cylindrical shaped narrow channel is formed. Subsequently, the cavity shape close to the bullet becomes nearly spherical due to rapid tumbling of the bullet, the cavity diameter reaches its maximum value when the bullet has tumbled through 90 ° in the gelatin at which instant it experiences the maximum resisting force of about 12 kN. The bullet tumbled through almost 180° in the vertical plane before it exited the gelatin.

The computed and the experimentally observed cavity profiles and cavity diameters at different times are displayed in Fig. 12. The computed penetration depth of 121 mm at 0.2 ms differs from the experimental value of 117 mm by only 3.4%. The bullet tumbling at 0.4 ms by ~90°after penetrating into the gelatin captured by the high-speed cameras is also well reproduced in the numerical solution. The computed bullet exit time of 0.6 ms agrees well with the experimental one, and the test and the computed diameters of the narrow channel differ from each other by about 12%. After the bullet has exited from the gelatin the experimentally seen expansion of the cavity in both radial and axial directions is well captured in the simulations, and the experimental and the computed diameters of the cavity are found to be close to each other. Thus the computational model reasonably well predicts deformations of the gelatin and of the bullet.

4.2. Pressure time histories

The shock pressure wave is an important ballistic characteristic in impact and penetration problems. The rapid increase and decrease of the pressure amplitude at a point can induce local compressive and tensile deformations in the gelatin. In simulations the pressure was measured at five points, A, B, C, D and E, situated on a plane passing through the line parallel to the direction of impact and that is 60 mm away from the impact point; see Fig. 11. The distance between any two adjacent points is 50 mm. Time histories of the pressure are exhibited in Fig. 13. Upon impact a shock wave is generated that propagates both radially and axially. The first peak pressures at points A through E have values 1.17, 1.15, 0.96, 0.86 and 0.6 MPa, respectively. At each one of these five points, the pressure sharply rises in about 20 µs, and the peak in the pressure is followed by a series of small amplitude oscillations due to the interaction between the bullet and the gelatin, and also between the incident wave and waves reflected from boundaries of the gelatin block. A second peak in the pressure at points C, D and E is most likely due to tumbling motion of the bullet. It is interesting to note that the peak pressure ~3 MPa at approximately 4 ms after impact occurs essentially when the bullet tumbles through 90° (see Fig. 12).

In order to qualitatively compare the computed and the experimental results, we have included in Fig. 13 experimental data of Huang et al. (2013). They observed similar “two peaks” in time histories of the pressure for the penetration of a 5.56 mm×45 mm rifle bullet into a

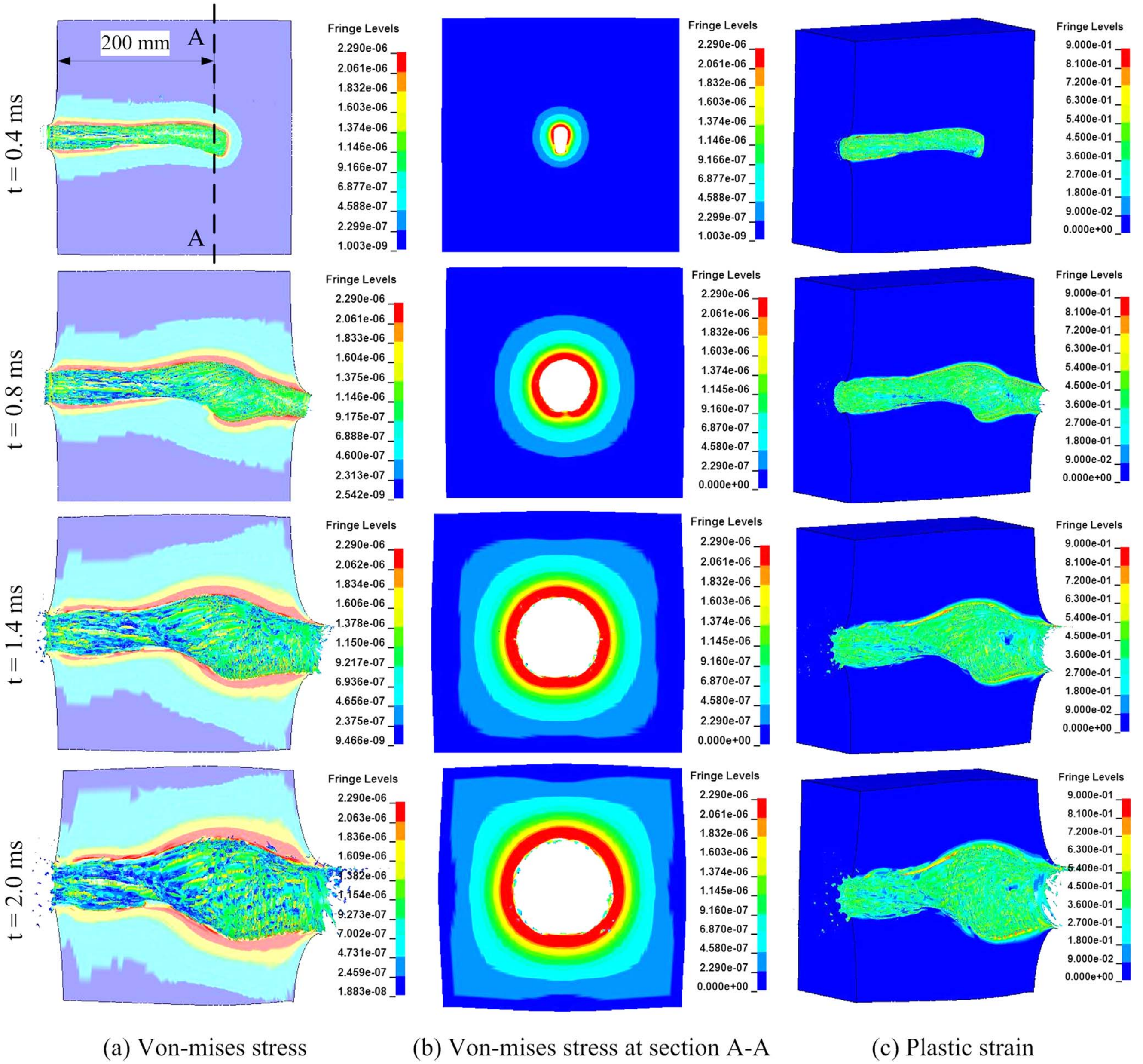

Fig. 14. For t=0.4, 0.8, 1.4 and 2 ms, contours of the von Mises stress (10^5 MPa) and of the effective plastic strain in the gelatin.

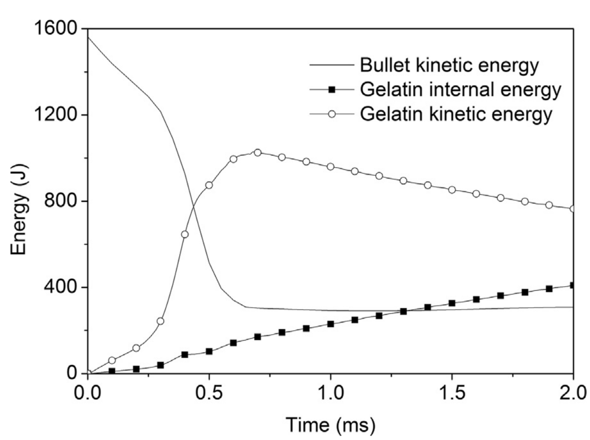

Fig. 15. Time histories of kinetic energies of the bullet and the gelatin, and of the internal energy of the gelatin.

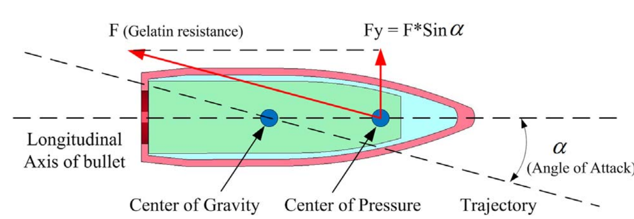

Fig. 16. Free body diagram of the bullet immersed in the gelatin.

block of gelatin with the five pressure sensors located at positions close to those in Fig. 11. They measured a pressure of about 2 MPa for the first peak and 6 MPa for the second peak. These results suggest that the presently computed pressure histories are reasonable.

4.3. Contours of the von Mises stress and the effective plastic strain

For four values of time, contours of the von Mises stress and of the effective plastic strain in a small region of the gelatin adjacent to the cavity surface are displayed in Fig. 14. Also exhibited are contours of the von Mises stress on the cross-section AA situated 200 mm from the impacted surface. The size of the plastically deformed region increases around the cavity surface as the cavity expands radially and axially. At t=0.4 ms, the cavity just reaches the cross-section AA and its shape is that of a bullet with its nose pointing downwards. At subsequent times of 0.8, 1.4 and 2.0 ms, the cavity shape at the cross-section AA is circular and the von Mises stress at points close to the cavity surface is a little above the initial yield stress of 0.2 MPa and the effective plastic strain there equals ~0.5. The region of high effective plastic strain extends to points approximately 8 mm in the radial direction from the cavity surface, and most of the gelatin is elastically deformed. We note that for values of material parameters listed in Table 1, the gelatin in a simple tension test begins to yield at an axial strain of 0.258.

4.4. Time histories of energies

Time histories of the KEs of the bullet and the gelatin, and of the strain energy of the gelatin are exhibited in Fig. 15. It is clear that the bullet KE curve has inflection points at about 0.3 and 0.6 ms. The bullet KE is reduced from 1,562 J at the instant of impact to 1,285 J after penetration into the gelatin for 0.25 ms and the formation of a narrow channel in the bullet. The KE rapidly decreases from 0.25 ms to 0.7 ms by which time the bullet KE equals 320 J. At 0.7 ms the bullet exited the gelatin with the residual KE of 304 J. Thus approximately 81% of the KE of the bullet was delivered to the gelatin block. The gelatin KE curve also has two inflection points that approximately correspond to those in the bullet KE curve. The maximum value, 1,025 J, of the gelatin KE occurs at about 0.7 ms. Subsequently the KE of the gelatin is converted into energy of elastic and plastic deformations of the gelatin, denoted in Fig. 15 by the gelatin internal energy. The internal energy of the gelatin monotonically increases in the time range for which we studied its deformations.

4.5. Effect of the angle of attack of the rifle bullet

The location in the gelatin of the maximum diameter of the cavity coincides with the bullet position where it tumbles through 90°. The corresponding computed penetration depths for angles of attack of 1°, 2° and 3°, with other parameters kept fixed, are 217, 188 and 171 mm respectively. These reveal that the penetration depth till the moment of the bullet tumbling through 90° decreases with an increase in the angle of attack. Taking the penetration depth for the angle of attack equal to 2° as the reference, the ± 1° change in the angle of attack alters the penetration depth by -9% and +15%.

The angle of attack equals the angle between the bullet velocity and its longitudinal axis. A free body diagram of the bullet displayed in Fig. 16 suggests that the component F_y of the resisting force acting on the bullet rotates it about an axis perpendicular to the bullet longitudinal axis. Taking α =2° as the reference, the ± 1° change in the angle of attack alters F_y by ± 50%. Thus a small change in the angle of attack significantly affects the tumbling and the penetration depth of the bullet. Of course, for larger reference values of α, a small change in its value will have a smaller effect on F_y.

The computed time histories of the bullet speed for the three values of α revealed that in each case the bullet speed rapidly decreases after 0.2 ms, and at t=1 ms the bullet residual velocities equal 271, 223 and 197 m/s, respectively, for α = 1°, 2° and 3°. It suggests that more of the bullet KE is transferred to the gelatin with an increase in the angle of attack.

5. Conclusions

Impact experiments involving the penetration of a rifle bullet into a block of ballistic gelatin were conducted, and the commercial finite element software, LS-DYNA, was used to simulate the test configurations. Images recorded with two cameras in the vertical and the horizontal directions were used to visualize the temporary cavity profiles. The ballistic gelatin was modeled as an elastic-plastic linearly strain hardening material with a polynomial equation of state. The computed penetration depth and cavity profiles are found to be close to those observed experimentally. The hydrostatic pressure at points close to the region where the bullet tumbles has "two peaks", the first is due to the initial impact of the bullet penetration and the second is due to the tumbling motion of the bullet in the gelatin. The plastic deformations occurred in a narrow, approximately 8 mm thick, region around the cavity surface with most of the gelatin undergoing only elastic deformations. The angle of attack is found to significantly affect the penetration depth when the bullet tumbles through 90°. The kinetic energy of the bullet transferred to the gelatin due to tumbling increases with an increase in the angle of attack of the bullet. The closeness of the test findings to the computed results imply that the computational model can reasonably well predict significant features of the impact event.

Acknowledgements

Authors thank Haosheng Wang, Bin Qin, Hailin Cui and Wenmin Yan of No.208 Research Institute of China Ordnance Industries for their help in conducting the experiments. This work, except for that of RCB, was supported by the National Natural Science Foundation of China (Grant No.11502119).

References

Aihaiti, M., Hemley, R.J., 2008. Equation of State of Ballistic Gelatin (II) [55048-EG.1]. Carnegie Institute of Washington.
Anderson, C.E., Jr, Holmquist, T.J., 2013a. Application of a computational glass model to compute propagation of failure from ballistic impact of borosilicate glass targets. Int. J. Impact Eng. 56, 2–11.
Anderson, C.E., Jr, Holmquist, T.J., 2013b. Computational modeling of failure for hypervelocity impacts into glass targets. Procedia Eng. 58, 194–203.
Antoine, G.O., Batra, R.C., 2016. Effect of curvature on penetration resistance of polycarbonate panels. J. Appl. Mech. 83, [Article No. 121002; DoI: 10 1115/ 1.4034520].
Appleby-Thomas, G.J., Hazell, P.J., Wilgeroth, J.M., Shepherd, C.J., Wood, D.C., Roberts, A., 2011. On the dynamic behavior of three readily available soft tissue simulants. J. Appl. Phys., 109, [Art. No. 0847011].
Batra, R.C., Kim, C.H., 1990. Effect of Viscoplastic Flow Rules on the Initiation and Growth of Shear Bands at High Strain Rates. J. Mech. Phys. Solids 38, 859–874.
Batra, R.C., Chen, X., 1994. Effect of frictional force and nose shape on axisymmetric deformations of a thick thermoviscoplastic target. Acta Mech. 106, 87–105.
Chadegani, A., Iyer, K., Mehoke, D., Batra, R.C., 2015. Hypervelocity impact of a steel microsphere on fused silica sheets. Int. J. Impact Eng. 80, 116–132.
Chen, X., Batra, R.C., 1993. Effect of frictional force on the steady state axisymmetric deformations of a viscoplastic target. Acta Mech. 97, 153–168.
Cronin, D.S., Falzon, C., 2010. Characterization of 10% ballistic gelatin to evaluate temperature, aging and strain rate effects. Exp. Mech. 51, 1197–1206.
CroninDS.Ballistic Gelatin Characterization and Constitutive Modeling. In: 2011 Annual Conference on Experimental and Applied Mechanics. Connecticut, USA; 2011. p.51-55.
CroninD.S., FalzonC.Dynamic characterization and simulation of ballistic gelatin. In: SEM Annual Conference and Exposition on Experimental and Applied Mechanics. Albuquerque, USA; 2009, p. 856-861.
Hallquist, J.O., 2012. LS-DYNA Keyword User's Manual,Version 971. Livermore Software Technology Corporation, LSTC, Livermore.
Huang, S., Wang, H.S., Wang, S., et al., 2013. Experimental study on pressure-wave characters in the process of typical small-caliber bullet penetrating gelatin. J. Ballist. 25 (1), 62–67.
Hub, J., Komenda, J., Novak, M., Expansion limit estimation of pistol hollow point bullet penetrating the block of substitute material. In: Nasprstek, J., Fischer, C. (Ed.), Proceedings of the 18th International Conference Engineering Mechanics 2012, Svratka, Czech Republic, p. 453-460.
Johnson, A.F., Holzapfel, M., 2003. Modelling soft body impact on composite structures. Compos. Struct. 61, 103–113.
Johnson, A.F., Holzapfel, M., 2006. Numerical prediction of damage in composite structures from soft body impacts. J. Mater. Sci. 41, 6622–6630.
Jussila, J., 2004. Preparing ballistic gelatine–review and proposal for a standard method. Forensic Sci. Int. 141, 91–98.
Kneubuehl, B.P., 2011. Wound Ballistics: Basics and Applications 4th ed.. Springer-Verlag, Berlin.
KoeneL., PapyA., 2010. Experimental and numerical study of the impact of spherical projectiles on ballistic gelatin at velocities up to 160 m/s. In: Proceedings of the 25th

International Symposium on Ballistics. Beijing, China. p. 1573–1579.
Kwon, J., Subhash, G., 2010. Compressive strain rate sensitivity of ballistic gelatin. J. Biomech. 43, 420–425.
Maiden, N., 2009. Historical overview of wound ballistics research. Forensic Sci. Med. Pathol. 5, 85–89.
MoyP., FosterM., GunnarssonC.A., WeerasooriyaT., 2010. Loading Rate Effect on Tensile Failure Behavior of Gelatins under Mode I. In: SEM Annual Conference on Experimental and Applied Mechanics. Indianapolis, USA, pp. 15–23.
Nagayama, K., Mori, Y., Motegi, Y., Nakahara, M., 2006. Shock hugoniot for biological materials. Shock Waves 15, 267–275.
NicholasNC, WelschJR.Institute for Non-Lethal Defense Technologies Report: Ballistic Gelatin. ADA446543; 2004.
Richler, D., Rittel, D., 2014. On the testing of the dynamic mechanical properties of soft gelatins. Exp. Mech. 54, 805–815.
Salisbury, C.P., Cronin, D.S., 2009. Mechanical properties of ballistic gelatin at high deformation rates. Exp. Mech. 49, 829–840.
Shen, W.X., Niu, Y.Q., Bykanova, L., Laurence, P., Link, N., 2010. Characterizing the interaction among bullet, body armor, and human and surrogate targets. J. Biomech. Eng. 132, 1–11.
Wang, Z.L., Konietzky, H., Huang, R.Y., 2009. Elastic–plastic-hydrodynamic analysis of crater blasting in steel fiber reinforced concrete. Theor. Appl. Fract. Mech. 52, 111–116.
Wen, Y.K., Xu, C., Wang, S., et al., 2015. Analysis of behind the armor ballistic trauma. J. Mech. Behav. Biomed. Mater. 45, 11–21.
Wen, Y.K., Xu, C., Wang, H.S., Chen, A.J., Batra, R.C., 2013. Impact of steel spheres on ballistic gelatin at moderate velocities. Int. J. Impact Eng. 62, 142–151.
WilbeckJS.Impact behaviour of low strength projectiles. Air Force MaterialsLaboratory, Technical Report AFML-TR-77-134, 1978.
Yoon, G.H., Mo, J.S., Kim, K.H., et al., 2015. Investigation of bullet penetration in ballistic gelatin via finite element simulation and experiment. J. Mech. Sci. Technol. 29 (9), 3747–3759.